

AD-A064 817

GEORGIA INST OF TECH ATLANTA SCHOOL OF ELECTRICAL EN--ETC F/G 17/9  
PARAMETRIC INVESTIGATION OF RADOME ANALYSIS METHODS.(U)

NOV 78 G K HUDDLESTON, H L BASSETT

AFOSR-77-3469

UNCLASSIFIED

AFOSR-TR-79-0068

NL

1 OF 1  
ADA  
064817



END  
DATE  
FILMED

4-79

DDC

AFOSR-TR- 79-0068

⑨ LEVEL II

ADA064817

PARAMETRIC INVESTIGATION  
OF  
RADOME ANALYSIS METHODS

By

G. K. Huddleston, H. L. Bassett, & J. N. Newton

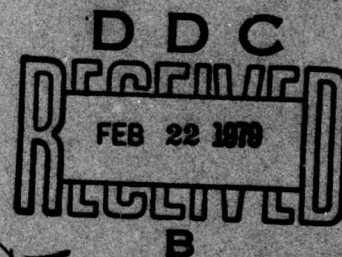
Prepared for

AIR FORCE OFFICE OF SCIENTIFIC RESEARCH (AFSC)  
BOLLING AIR FORCE BASE, D. C. 20332

*see 1477  
in  
back*

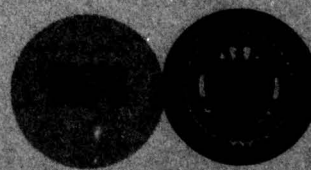
ANNUAL TECHNICAL REPORT  
GRANT AFOSR-77-3469  
1 October 1977 - 30 September 1978

November 1978



*Q7*

GEORGIA INSTITUTE OF TECHNOLOGY  
SCHOOL OF ELECTRICAL ENGINEERING  
ATLANTA, GEORGIA 30332



AIR FORCE OFFICE OF SCIENTIFIC RESEARCH (AFSC)  
NOTICE OF TRANSMITTAL TO DDC

DDC FILE COPY

PARAMETRIC INVESTIGATION  
OF  
RADOME ANALYSIS METHODS

by

G. K. Huddleston, H. L. Bassett, and J. N. Newton

for

Air Force Office of Scientific Research  
Bolling Air Force Base, D.C. 20332

Under

Grant AFOSR-77-3469  
October 1, 1977 - September 30, 1978

School of Electrical Engineering  
and  
Engineering Experiment Station

Georgia Institute of Technology  
Atlanta, Georgia 30332

November 1978

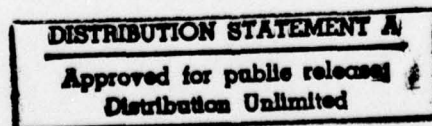
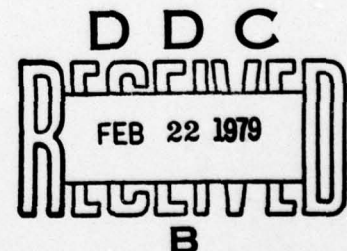


# TABLE OF CONTENTS

	<u>PAGE</u>
I. Introduction and Summary . . . . .	1
II. Progress to Date . . . . .	2
III. Presentations and Publications . . . . .	22
IV. Personnel and Interactions . . . . .	22
V. References . . . . .	23
APPENDIX A . . . . .	25

ACCESSION for		
NTIS	White Section	<input checked="" type="checkbox"/>
DDC	Buff Section	<input type="checkbox"/>
UNANNOUNCED		<input type="checkbox"/>
JUSTIFICATION _____		
BY _____		
DISTRIBUTION/AVAILABILITY CODES		
Dist.	Full and/or	SPECIAL
A		

# LIST OF ILLUSTRATIONS

<u>FIGURE</u>		<u>PAGE</u>
1	Illustration of the Fast Receiving Method of Radome Analysis . . . . .	8
2	Plane Wave Propagation Through An Infinite Plane Sheet . . . . .	9
3	Geometry and Dimensions of Small Radome Showing Orientation of Small Antenna . . . . .	12
4	Geometry and Dimensions of Medium Size Radomes Having Fineness Ratios of 1:1, 1.5:1, and 2:1 Showing Small, Medium, and Large Antennas . . . . .	13
5	Geometry and Dimensions of Large Radome Showing Orientations of Small, Medium, and Large Antennas . . . . .	14
6	Photographs of Two Rexolite Radomes Having Fineness Ratio of 1:1 . . . . .	17
7	Geometry and Dimensions of Three Monopulse Antennas for Use at 35 GHz . . . . .	18
8	Photographs of Antennas and Mounting Fixture . . . . .	20

# LIST OF TABLES

<u>TABLE</u>		<u>PAGE</u>
1	Accuracy and Computation Time for Surface Integration Method . . . . .	6
2	Radome Dimensional Data in Wavelengths . . . . .	15
3	Ratios of $D_{is}/D_{ap}$ for Selected Antennas and Radomes . . . . .	21

## PARAMETRIC INVESTIGATION OF RADOME ANALYSIS METHODS

### I. Introduction and Summary

The overall objective of this research is to develop a general theory of radome analysis and to determine the accuracies of various radome analysis methods under controlled conditions of antenna size and placement, wavelength, and radome size and shape. Experimental measurements on selected antenna/radome combinations at 35 GHz will be used as true data in the assessment of accuracy.

During the first year, which this report covers, a general theory of analysis has been developed based on the Lorentz reciprocity theorem and on the Huygens-Fresnel principle. Computer-aided methods of analysis based on these principles have been formulated and programmed. Three monopulse antennas have been designed and fabricated for use in carrying out the measurements at 35 GHz. Three radomes have been designed and fabricated for use in the experimental program. A mechanical fixture has been fabricated which will allow accurate positioning of the antenna with respect to the radome and with respect to the reference system used for pattern measurements. A detailed discussion of the progress in the first year is presented in Section II below.

During the second year, the initiation efforts of the first year's work will come to fruition through concentrated experimental and analytical efforts to gather true and calculated data which will serve as the basis for realizing the overall research objective. Extensive pattern measurements will be made for nine of the fifteen antenna/radome combinations

available. These experimental efforts will be paralleled by computer-aided analyses of the same combinations for comparison purposes. In addition, techniques to account for the effects of metal tips will be incorporated into the analysis methods for use during the third and final phase of the research.

In the third year, it is anticipated that measurements will be carried out on radomes to which metal tips have been added, and comparisons to theoretical predictions will be made. In addition, antenna/radome configurations which lend themselves to exact analysis using boundary-valued approaches and variational and relaxation techniques will be investigated.

Two publications and three presentations concerning this research have resulted. They are described in Section III along with papers planned for submission to technical journals.

The professional personnel associated with the research effort are listed in Section IV.

Appendix A contains copies of the two papers presented at symposia.

## II. Progress to Date

Efforts during the first year's work have been devoted to developing the general theory of radome analysis, formulating the radome analysis methods, implementing the methods in digital computer software, designing and building three monopulse antennas, designing five suitable radomes, and designing and fabricating a test fixture for positioning the antenna/radome combinations in the measurement environment. These efforts have

been carried out to prepare for the extensive measurements and analytical efforts planned for Phase II.

The general theory of radome analysis is based on the Lorentz reciprocity theorem [1] and the Huygens-Fresnel principle [2] as described in the papers included in Appendix A. Briefly, the reciprocity theorem serves as the basis for all receiving formulations of radome analysis; i.e., the response of the antenna inside the radome to a plane wave incident on the radome is the desired analysis objective. The Huygens-Fresnel principle serves as the basis for all rigorous transmitting formulations; i.e., the Fraunhofer fields are determined for the case when the radome-enclosed antenna is radiating by performing integrations of the tangential electric and magnetic fields over a surface which encloses the sources. Since a homogeneous medium is required by the theory in the region not containing the sources, the radome must also be enclosed by the surface. The third facet of the general theory makes use again of the reciprocity theorem for widely separated antennas to provide the unifying connection between the response of an antenna to a plane wave of specified polarization and direction of arrival and the vector far fields of the antenna.

Analytical efforts thus far have concentrated on formulating and implementing both receiving and transmitting formulations which require integration of the fields over the outer surface of the radome. Upon examination of the role of the field scattered by the radome when a plane wave is incident, it has been established that the scattered field contributes nothing to the antenna response and, therefore, can be neglected in the computations. The equivalence of the transmitting and receiving

formulations has also been rigorously established for the first time, the import of which is that intermediate calculations of the vector far field as required in the transmitting case can be avoided in many cases of practical importance.

Attention has also been directed toward sampling of the electromagnetic fields on the surface of the radome as required in the surface integrations. Two methods have been considered. In the first, the radome surface is partitioned into elemental areas by dividing the axis of symmetry ( $z_R$ -axis) into equal linear increments; in the circumferential direction, equal angular segments are used. In the second method, equal angular increments are used in the longitudinal ( $\theta$ ) direction so that the length of the elemental area is the same regardless of location on the surface. Angular increments are also used in the circumferential ( $\phi$ ) direction and are adjusted so that at the center of the elemental area, the arc distance is approximately constant. In both methods, the field values are computed at the center of each elemental area.

The surface integration method has been implemented in computer software (Fortran IV) and is currently being tested for accuracy and speed of computation. A simple method has been devised to do this as follows. A tangent ogive radome shape having zero wall thickness represents the surface of integration. The tangential components of a source field  $\underline{E}_s$ ,  $\underline{H}_s$  are specified over the circular region or aperture at the base of the radome. A plane wave relationship is assumed between  $\underline{E}_s$  and  $\underline{H}_s$ , where the direction of propagation is normal to the circular region; i.e., parallel to the axis of symmetry of the radome. A plane wave having specified polarization and direction of arrival is assumed

incident on the circular aperture and, simultaneously, on the tangent ogive surface. The reaction integral [2] is proportional to the voltage received by the circular aperture antenna and is easily computed for the circular aperture to yield an exact result. The computation of the same received voltage is carried out using the computer-aided techniques for various tangent ogive surfaces.

Table I shows some salient results obtained with the computer-aided surface integration method. Five radome shapes (sizes) as explained below were used. The results shown were obtained using the second method of sampling described above. Sample distances (equal in  $\theta$  and  $\phi$ ) of  $\lambda/6$  to  $\lambda$  were used, where  $\lambda$  is the free space wavelength. The total number of samples depends on the sample increment and radome size as shown in column four of the table. Comparison of the true and computed values of received voltage shows excellent agreement. Examination of the entries in the last column of Table I shows the dramatic influence of the number of samples on computation time.

It can be concluded at this point that the surface integration may be practical for small radomes but perhaps not so practical for larger radomes, assuming that a fixed sample size which yields consistently accurate results can be established. But this trend is neither unexpected nor catastrophic from a practical standpoint. It is expected that the other computational methods under investigation will yield acceptably accurate results for large radomes and will require much less computation time; in fact, the larger the radome and antenna, the more accurate will be the computed result. The question addressed by this research concerns, of course, the establishment of the ranges of validities of these various

Table I. Accuracy and Computation Time for  
Surface Integration Method

Radome ID				Received Voltage		
Diameter ( $\lambda$ )	Length ( $\lambda$ )	Sample Size	Number of Samples	True	Computed	Computation Time (sec)
20.49	19.93	$\lambda/6$	35157	-1.28355	-1.28355	61.11
20.49	19.93	$\lambda/3$	8718	-1.28355	-1.28362	13.05
20.49	19.93	$\lambda/2$	3869	-1.28355	-1.28373	7.00
20.49	19.93	$\lambda$	967	-1.28355	-1.28431	1.64
11.86	22.30	$\lambda/6$	20716	-0.43011	-0.43011	31.68
11.86	22.30	$\lambda/3$	5167	-0.43011	-0.43013	7.95
11.86	22.30	$\lambda/2$	2262	-0.43011	-0.43017	4.05
11.86	22.30	$\lambda$	571	-0.43011	-0.43037	.86
11.86	16.78	$\lambda/6$	15929	-0.43011	-0.43011	24.68
11.86	16.78	$\lambda/3$	3973	-0.43011	-0.43015	6.77
11.86	16.78	$\lambda/2$	1769	-0.43011	-0.43021	2.59
11.86	16.78	$\lambda$	442	-0.43011	-0.43054	.82
11.86	11.30	$\lambda/6$	11554	-0.43011	-0.43012	19.69
11.86	11.30	$\lambda/3$	2846	-0.43011	-0.43019	5.31
11.86	11.30	$\lambda/2$	1265	-0.43011	-0.43031	2.31
11.86	11.30	$\lambda$	319	-0.43011	-0.43092	.61
7.56	6.97	$\lambda/6$	4560	-0.17480	-0.17482	7.11
7.56	6.97	$\lambda/3$	1115	-0.17480	-0.17489	2.37
7.56	6.97	$\lambda/2$	498	-0.17480	-0.17502	1.06
7.56	6.97	$\lambda$	127	-0.17480	-0.17567	.25

methods.

One of the speedier radome analysis methods under investigation uses a receiving formulation as described earlier [3]. The method is illustrated in Figure 1. The plane wave  $\underline{E}_i, \underline{H}_i$  is incident on the radome with direction of arrival  $\hat{k}_a$ . A ray is traced backwards from each aperture point  $(x,y,0)$  in the direction  $\hat{k}_a$  to find the intersection with the radome wall and the unit normal vector  $\hat{n}_R$  at the intersection point. From  $\hat{k}_a, \hat{n}_R$ , and  $\underline{E}_i$ , the field  $\underline{E}_R$  produced on the antenna aperture can be found, where the components of  $\underline{E}_i$  parallel and perpendicular to the plane of incidence are properly weighted by the complex transmission coefficients  $T_1, T_{11}$  as illustrated in Figure 2.

The transmission coefficients used are those which apply to an infinite plane dielectric sheet [4]. This approximate method of transforming the fields on one side of the radome wall to the other side appears to be a common feature of all radome analysis methods except that described by Van Doeren [5]. Use of this method precludes the computation of surface (trapped) wave effects and may represent the single most significant deficiency in all of these methods.

Another computationally fast method under investigation utilizes a transmitting formulation and makes extensive use of the Fast Fourier Transform (FFT) to enhance the computational speed [6]. Briefly, the radiation from the antenna is characterized by using the plane wave spectrum (PWS) representation (a modal expansion) [7]. The antenna aperture is sampled at an array of equally spaced points in  $x$  and  $y$ . From each point in the aperture there emanates a spectrum of plane waves, obtained very simply as the (inverse) FFT of the tangential electric

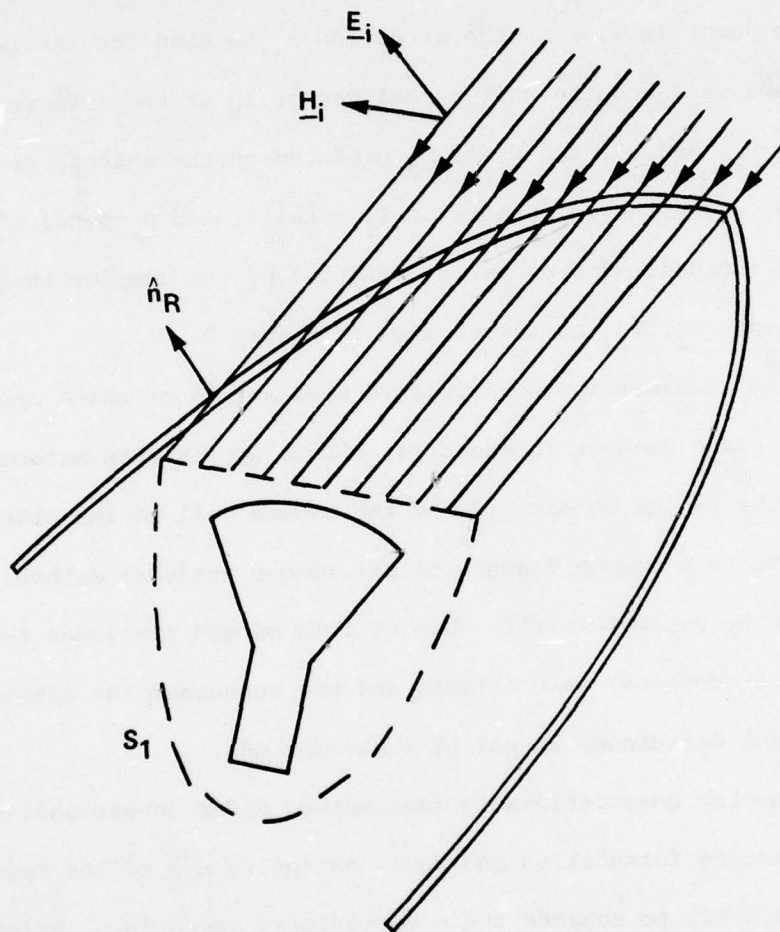


Figure 1. Illustration of the Fast Receiving Method of Radome Analysis

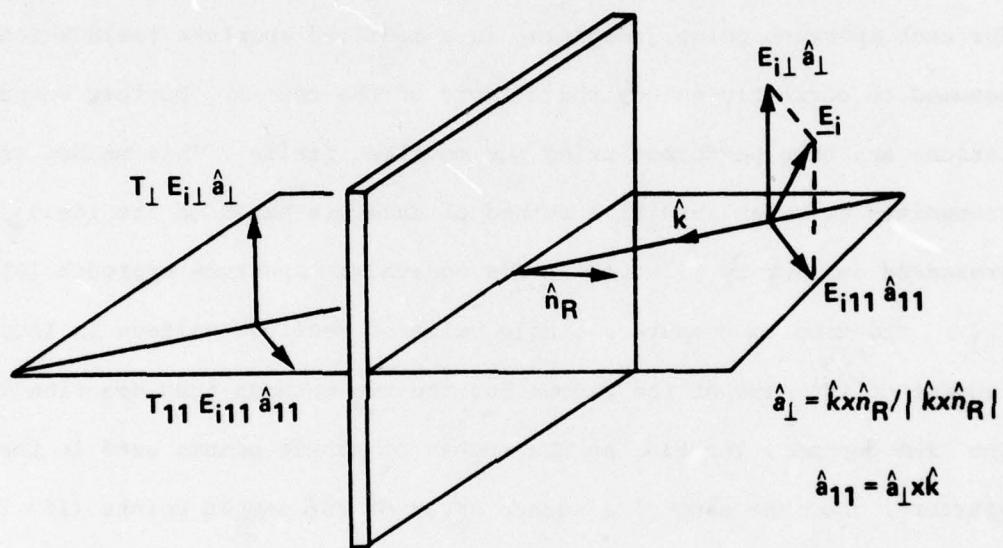


Figure 2. Plane Wave Propagation Through an Infinite Plane Sheet

field in the aperture. Rays are traced to each point to find their intersections with the inside surface of the radome. The plane wave field  $\underline{e}$ ,  $\underline{h}$  associated with each ray is weighted by the transmission coefficients  $T_1$ ,  $T_{11}$  as depicted in Figure 2. The modified plane wave  $\underline{e}'$ ,  $\underline{h}'$  is then included in the summation of all such contributions to produce modified aperture fields  $\underline{E}'_s$ ,  $\underline{H}'_s$  at the specified point. The procedure is repeated for each aperture point, resulting in a modified aperture field which is assumed to correctly embody the effects of the radome. Further computations are then performed using the modified fields. This method is recognized to be an intuitive method of analysis based on the ideas presented earlier by Kilkoynne in his equivalent aperture approach [8].

The time to compute a single value of received voltage is independent of the size of the radome for the two methods just described. The time depends, instead, on the number of sample points used in the aperture. For the case of a square array of 256 sample points (16 x 16), the computation time for one value of received voltage for the fast transmitting case is approximately one minute. The fast receiving method requires 1.5 seconds. No account is made here of the core memory requirements.

Some analytical work and associated computer implementation remains to be done. An additional receiving formulation method of analysis will be implemented wherein integration over the inner surface of the radome will be done to determine if any computational advantages are realized. Antenna characterization routines which utilize theoretical representation and measured data also being implemented. Of future interest is the spherical wave expansion described by Ludwig [9] where

limited measured far-field data are used to generate coefficients in the expansion so that radiation from the antenna can be more accurately described analytically. Presently, the PWS formulation is being used to characterize radiation from the antenna. Also, the effects of reflected waves are also to be included in the analysis using the Huygens-Fresnel formulation embodied in Equations (108) and (109) of Silver [2]. Finally, a method of comparison of analysis methods is being developed which includes both computation time and memory requirements so that fair comparisons can be made.

Five radomes have been designed for fabrication and use during the experimental program. All five radomes have the tangent ogive shape. Three radomes have 1:1 fineness ratios (length/diameter) and have dimensions to yield a small, medium, and large radome in terms of base diameter in wavelengths. Two other radomes have the medium-size base diameter but fineness ratios of 1.5:1 and 2:1.

The geometry and dimensions of the radomes showing the orientations of the antennas to be used with them are illustrated in Figures 3, 4, and 5. The radius of the generating arc is shown in each figure as  $R_{is}$ . The antenna is shown pivoted about a gimbal point to look in a direction that is  $15^\circ$  from the axis of symmetry of the radome. The dimension of a wavelength is indicated by  $\lambda$  in each figure for convenient reference. Table II presents the radome dimensions in terms of wavelengths at this frequency.

Two radomes have been fabricated using Rexolite ( $\epsilon_r = 2.52$ ). A full-wavelength wall thickness for this material at 35 GHz is approximately 0.25 inch. A full-wavelength thickness has been selected to

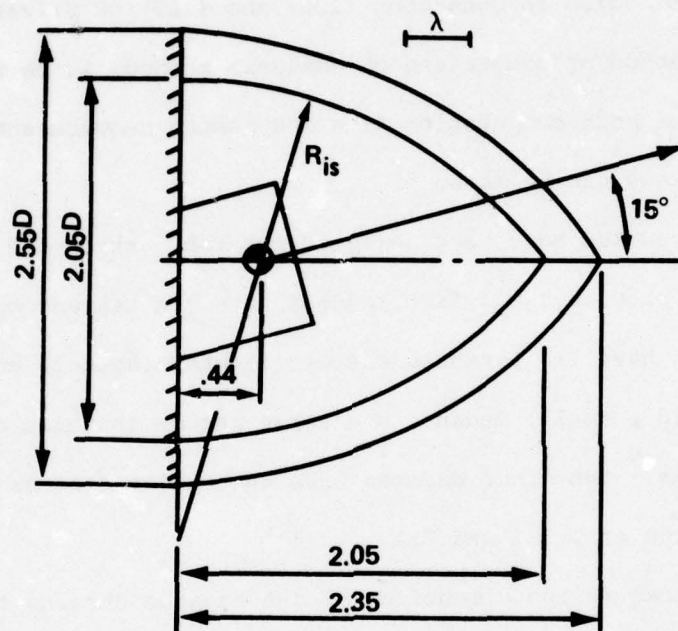


Figure 3. Geometry and Dimensions of Small Radome  
Showing Orientation of Small Antenna

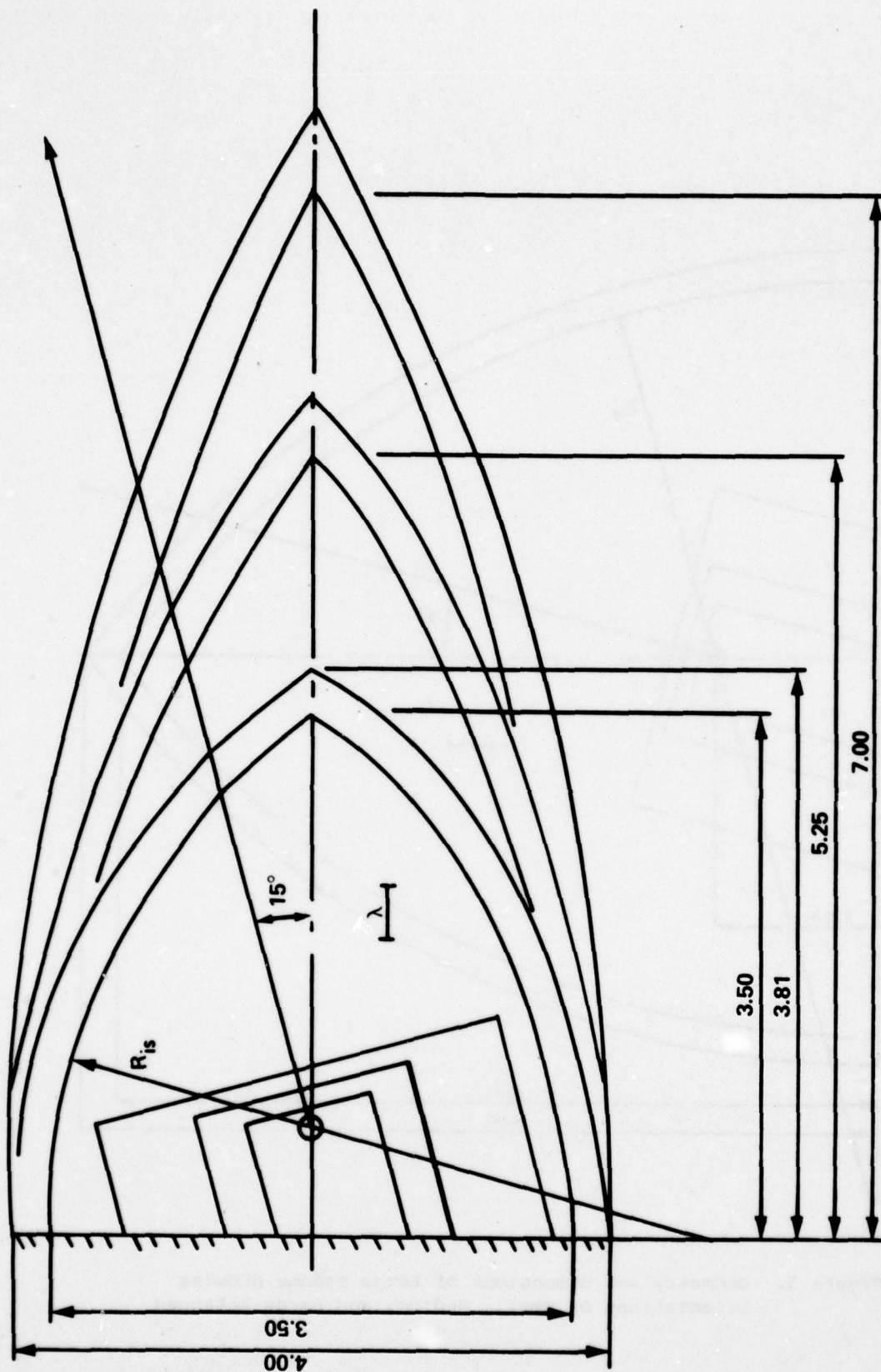


Figure 4. Geometry and Dimensions of Medium Size Radomes Having Fineness Ratios of 1:1, 1.5:1, and 2:1 Showing Small, Medium, and Large Antennas

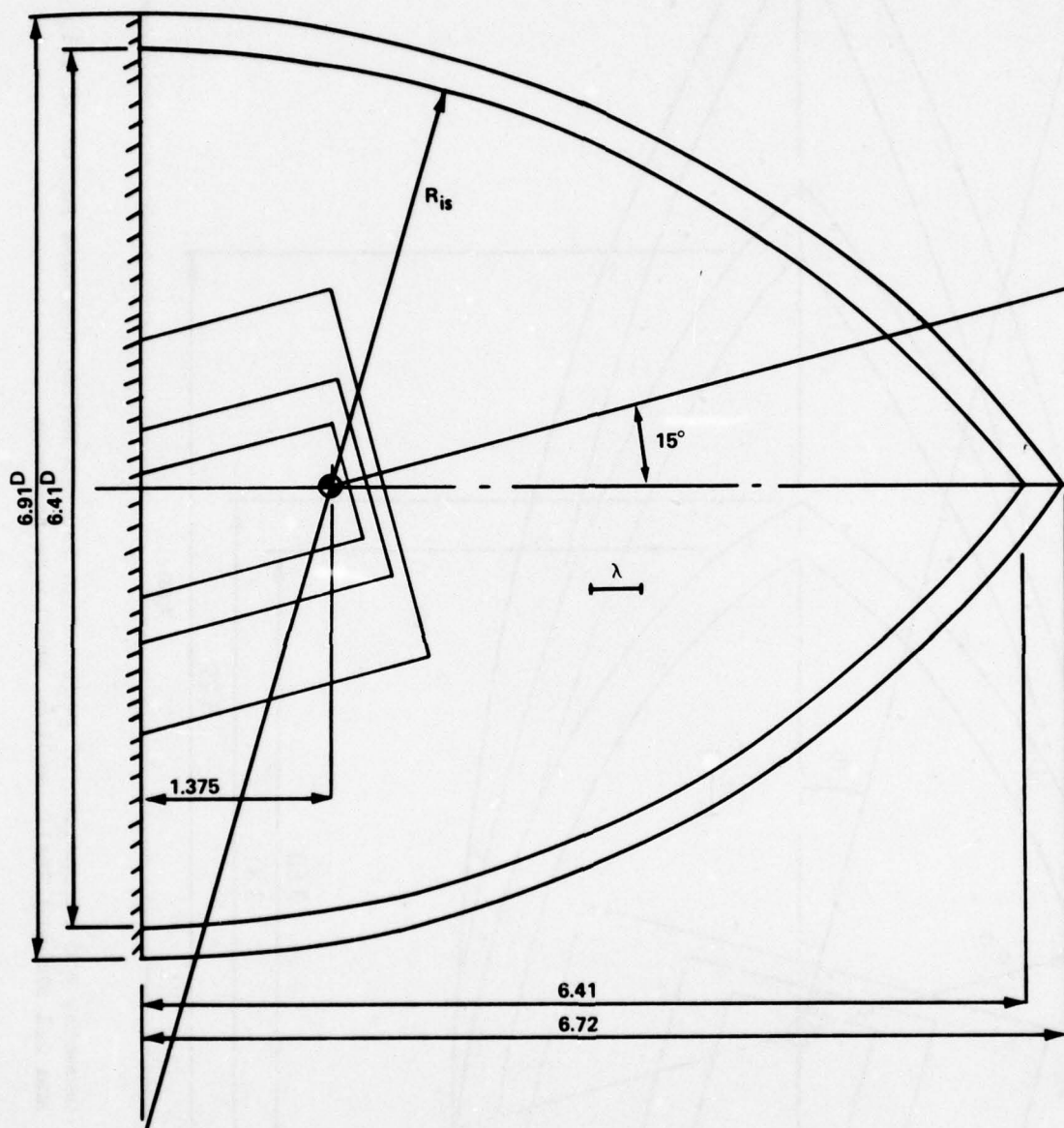


Figure 5. Geometry and Dimensions of Large Radome Showing Orientations of Small, Medium, and Large Antennas

Table II. Radome Dimensional Data in Wavelengths

	Inside Diameter	Inside Length	Outside Diameter	Outside Length
Small (F=1)	6.08	6.08	7.56	6.97
Medium (F=1)	10.38	10.38	11.86	11.30
Medium (F=1.5)	10.38	15.57	11.86	16.78
Medium (F=2.0)	10.38	20.76	11.86	22.30
Large (F=1)	19.01	19.01	20.49	19.93

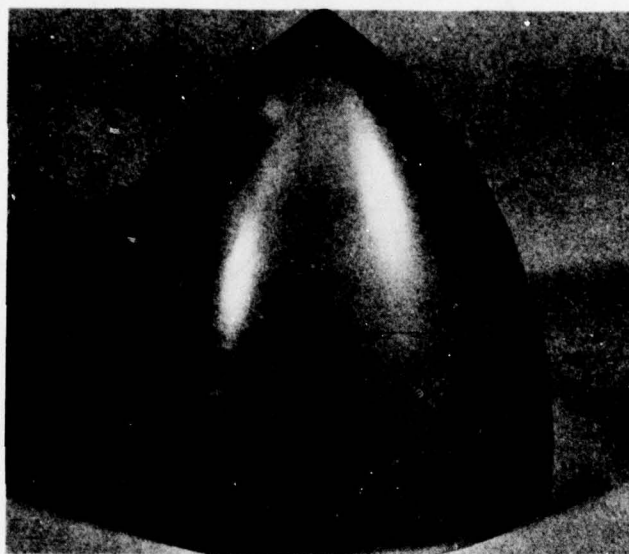
provide adequate strength and rigidity for the larger radomes and to provide consistent effects for all sizes. Rexolite has excellent electromagnetic and machining properties. Photographs of the two radomes are shown in Figure 6.

Three four-horn monopulse antennas, representing a small, medium, and large antenna, have been designed and fabricated for use alone and with the five radomes. Each antenna is connected through a circular-to-rectangular waveguide transition and adapter network to a monopulse comparator which forms sum, elevation difference, and azimuth difference channels as required in monopulse tracking. The waveguide transitions and adapter networks have been fabricated in the main campus machine shop. The four-horn configurations have been built and their aperture dimensions are illustrated in Figure 7. These antennas are designed to provide sum pattern beamwidths of  $8^\circ$ ,  $15^\circ$ , and  $30^\circ$ .

A mechanical fixture to position the radome with respect to the antenna and to position the combination in the pattern range coordinate system has also been built. Basically, a simple fixture is used which mounts on the azimuth positioner turntable and holds the antenna in a horizontal position. The antenna is mounted in a horizontal bushing so that accurate rotation of the antenna about its longitudinal axis is provided. If this axis is designated as the z-axis of the antenna, then rotation of the antenna about the z-axis selects a  $\phi = \text{constant}$  plane in the associated spherical coordinate system. Rotation of the entire assembly about the vertical axis of the positioner turntable corresponds to movement in the  $\theta$  direction of the spherical system. Vertical polarization corresponds to  $E_\theta$ , horizontal polarization corresponds to  $E_\phi$ .



(a) Small Radome



(b) Medium Radome

Figure 6. Photographs of Two Rexolite Radomes  
Having Fineness Ratio of 1:1

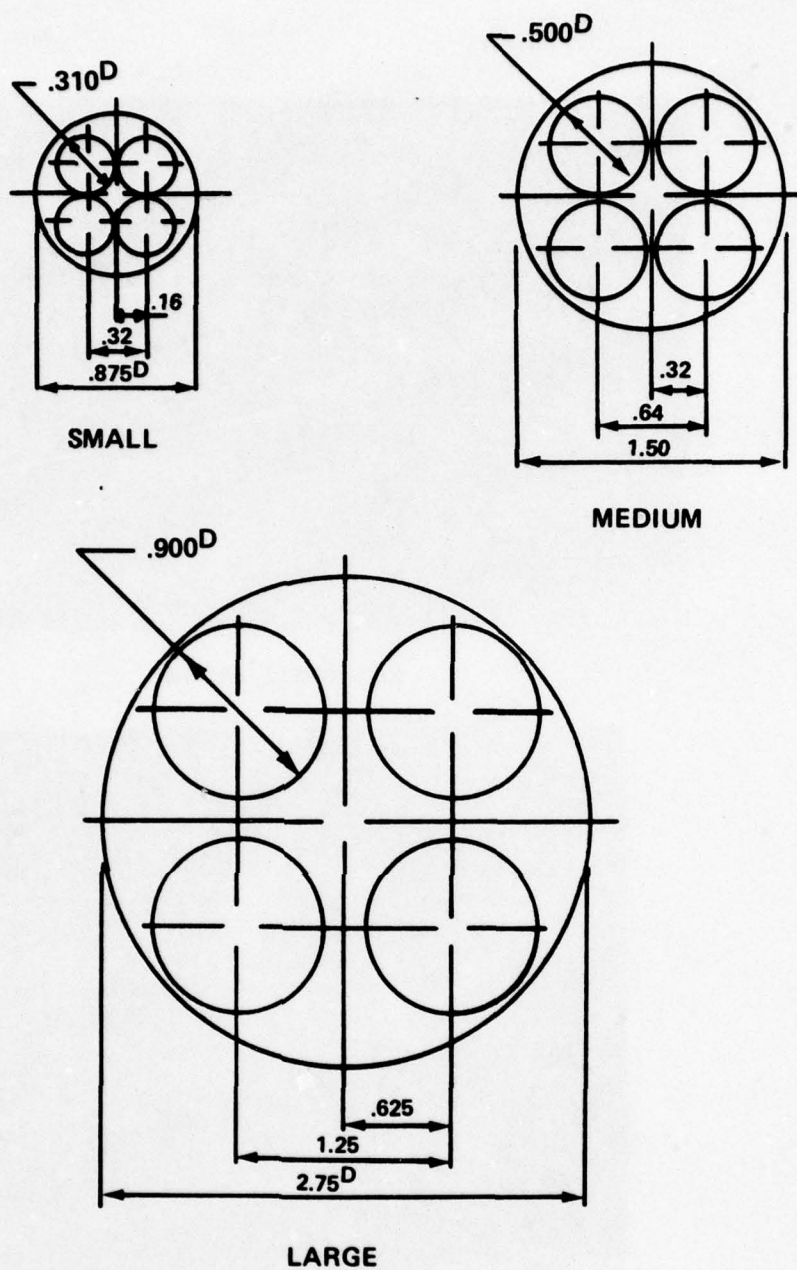
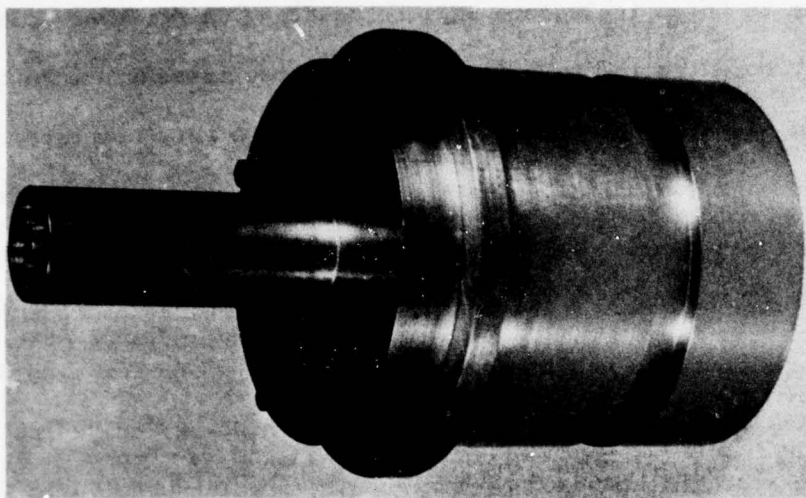


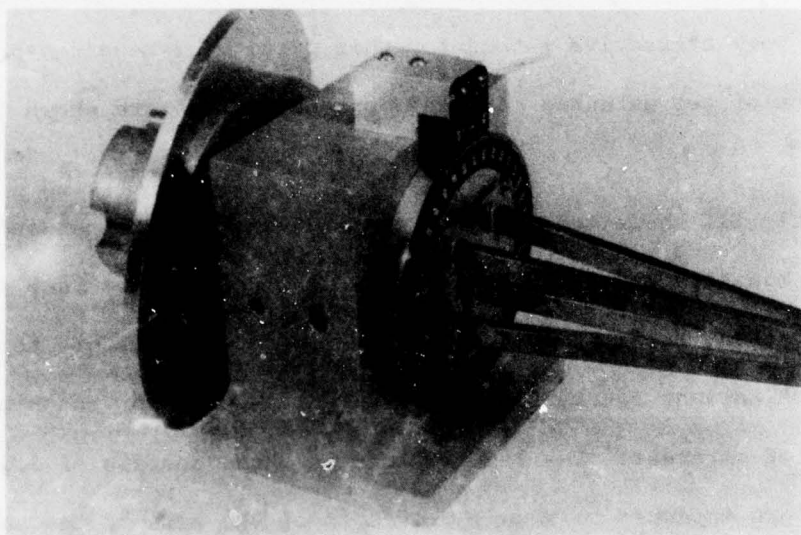
Figure 7. Geometry and Dimensions of Three Monopulse Antennas for Use at 35 GHz

The radome is positioned with respect to the antenna by a circular base plate to which the radome will be mounted. A circular hole has been accurately bored in the base plate which allows insertion onto the corresponding diameter antenna and which provides a very accurate, single angular orientation of the antenna z-axis with respect to the axis of symmetry of the radome. Rotation of the radome and base plate about the antenna z-axis provides selection of any desired plane of radome scan. Each antenna requires a different diameter base plate for each different radome with which the antenna is to be used; however, only nine such base plates are required and each base plate is very inexpensive to fabricate. Although this method of orienting the radome with respect to the antenna does not allow complete degrees of freedom, its low cost and high accuracy make it a very attractive method for this particular research program. Photographs of two antennas and the mounting fixture are shown in Figure 8.

Table III shows the specific combinations of antennas and radomes for which measured and analytical data will be obtained. Each entry in the table is the ratio of inside base diameter of the radome to the diameter of antenna aperture. Entries are made only for the nine combinations of interest. The results for the three entries of 2.33 for which  $F=1$  are expected to show the effects of the size of the antenna/radome combination in wavelengths on the accuracy of the analysis methods. Results for the other entries of 2.33 and  $F=1$  will provide information on the accuracy of the methods as a function of the relative size of antenna and radome. The entries of 2.33 for medium size radomes indicate those combinations which will provide information concerning the effects of



(a) Small Antenna



(b) Large Antenna

Figure 8. Photographs of Antennas and Mounting Fixture

Table III. Ratios of  $D_{is}/D_{ap}$  for Selected Antennas and Radomes.

Radome	Antenna		
	Small	Medium	Large
Small (F=1)	2.33	--	--
Medium (F=1)	3.98	2.33	1.27
Medium (F=1.5)	--	2.33	--
Medium (F=2.0)	--	2.33	--
Large (F=1)	7.28	4.27	2.33

fineness ratio on accuracy.

### III. Presentations and Publications

G. K. Huddleston, H. L. Bassett, and J. N. Newton, "Parametric Investigation of Radome Analysis Methods," presented at and published in the Proceedings of the 1978 International IEEE AP-S Symposium, pp. 199-202, May 1978; also presented at and published in the Proceedings of the Fourteenth Symposium on Electromagnetic Windows, pp. 53-55, June 1978, (Copies included in Appendix A).

G. K. Huddleston, "Radome Analysis," invited presentation to Atlanta Chapter of IEEE, AP-S/MTT Group, September 26, 1978.

G. K. Huddleston, "A General Theory of Radome Analysis," a paper planned for submission to IEEE Transactions on Antennas and Propagation, January 1979.

### IV. Personnel and Interactions

The following professional personnel are actively engaged in this research program:

G. K. Huddleston	Assistant Professor	School of Electrical Engineering
H. L. Bassett	Senior Research Engineer	Engineering Experiment Station
J. N. Newton	Research Engineer	Engineering Experiment Station

Dr. Huddleston and Mr. Bassett serve as co-principal investigators. Dr. Huddleston directs the analytical efforts while Mr. Bassett directs the experimental work. Mr. Jason Rusodimos, a graduate student in the School of Electrical Engineering works with Dr. Huddleston on the computer implementation of various analysis methods.

No specific interactions have taken place with other laboratories or DOD agencies; however, tentative plans have been made with Eglin Air Force Base (Dr. Ralph Calhoun, AFATL/DLMP) for the transfer of the analytical technology developed during this research.

V. References

1. R. E. Collin and F. J. Zucker, "Antenna Theory, Part 1," Sections 4.2 and 4.5, McGraw-Hill, New York, 1969.
2. Samuel Silver, ed., Microwave Antenna Theory and Design, Section 3-8, McGraw-Hill, New York, 1949.
3. G. K. Huddleston and E. B. Joy, "Development of Fabrication and Processing Techniques for Laser Hardened Missile Radomes: Radome Electrical Design Analysis," Technical Report for Martin-Marietta Aerospace, April 1977.
4. J. H. Richmond, "Calculation of Transmission and Surface Wave Data for Plane Multilayer and Inhomogeneous Plane Layers," Air Force Contract No. AF 33(615)-1081, Antenna Laboratory, Ohio State University, Columbus, Ohio, October 1963.
5. R. E. Van Doeren, "Application of the Integral Equation Method to Scattering from Dielectric Rings," Contract N62269-C-0582, Naval Air Development Center, Johnsville, PA, April 1968.
6. E. B. Joy and G. K. Huddleston, "Radome Effects on Ground Mapping Radar," Contract DAAH01-72-C-0598, U.S. Army Missile Command, March 1973.
7. Collin and Zucker, Ch. 3.
8. N. R. Kilcoyne, "An Approximate Calculation of Radome Boresight Error," Proceedings of the USAF/Georgia Tech Symposium on Electromagnetic Windows, pp. 91-111, June 1968.
9. A. C. Ludwig, "Near-Field Far-Field Transformations Using Spherical Wave Expansions," IEEE Transactions, AP-19, No. 2, pp. 214-220, March 1971.

APPENDIX A

Copies of Papers Presented

at

1978 International IEEE AP-S Symposium

and

Fourteenth Symposium on Electromagnetic Windows

## PARAMETRIC INVESTIGATION OF RADOME ANALYSIS METHODS

Presented at

1978 International IEEE AP-S Symposium  
University of Maryland  
College Park, Maryland  
May 1978

G. K. Huddleston, H. L. Bassett, and J. M. Newton  
Georgia Institute of Technology  
School of Electrical Engineering and Engineering Experiment Station  
Atlanta, Georgia 30332

Numerous methods of radome analysis have been developed, and some comparisons of theoretical and measured results have been made for specific radome/antenna combinations; however, no attempt has been made to define the ranges of antenna and radome parameters over which any given method of analysis yields acceptably accurate results. This paper describes some early results of an investigation recently undertaken to determine the accuracies of various radome analysis methods under controlled conditions of antenna size and placement, wavelength, and radome size and shape. A fundamental theory of radome analysis has been developed and is presented below. Comparisons of computed results obtained for two methods of analysis are also presented. No experimental results are available at this time, but rather extensive measurements involving antennas and radomes of various sizes are planned.

### Theory

The Lorentz reciprocity theorem [1] is a starting point for the formulation of a basic theory of radome analysis. Field equivalence principles [2] are also important in suggesting approximate methods of obtaining the fields called for in the reciprocity theorem; more importantly, such theory is needed to obtain the transmitting formulation for radome analysis.

Consider the antenna/radome combination shown in Figure 1 where the surface  $S$  encloses the antenna. Let a plane wave be incident on the radome from the direction  $\hat{K}_A$  expressed in the antenna coordinate system  $(X,Y,Z)$ . Then application of the reciprocity theorem results in the following expression for the voltage produced at the antenna terminals by the incident field:

$$V_R(\hat{K}_A) = C \iint_S (\underline{E}_T \times \underline{H}_R - \underline{E}_R \times \underline{H}_T) \cdot \hat{n} da \quad (1)$$

where  $C$  is a complex constant and where

$\underline{E}_T, \underline{H}_T$  = the electric and magnetic fields produced on S when the antenna is transmitting (and no fields are incident on the radome from the outside)

$\underline{E}_R, \underline{H}_R$  = the electric and magnetic fields produced on S when the plane wave is incident (and the antenna is passive or in the receive mode)

$\hat{n}$  = unit vector pointing out of the volume V enclosed by S

da = element of area on the surface S

The fields  $(\underline{E}_R, \underline{H}_R)$  and  $(\underline{E}_T, \underline{H}_T)$  are the total fields produced in each case and would correctly include incident and all scattered components. The voltage given by Equation (1) is exact and serves as a basic tenet of radome analysis theory. The surface S may be any conveniently chosen closed surface. Linear, homogenous, isotropic media are assumed. Time variations of the form  $e^{j\omega t}$  are understood and suppressed.

A second generalized approach to radome analysis uses a transmitting formulation which does not consider explicitly the fields produced by an incident plane wave. Instead, the tangential fields produced by the antenna on a closed surface outside the radome are used to determine the fields anywhere in the unbounded, homogeneous medium outside this surface. Equations (108) and (109) of [3] are the basic equations which apply, where the point P is at a great distance from S so that  $\underline{E}_P, \underline{H}_P$  become the far zone fields  $\underline{E}_{Tff}, \underline{H}_{Tff}$  radiated by the antenna in the presence of the radome. Selection of the surface S are the parameters which, again, differentiate the various methods of radome analysis based on a transmitting formulation.

The voltage that would be received by the antenna which produces far zone fields  $\underline{E}_{Tff}, \underline{H}_{Tff}$  is given by [4]

$$V_R(\hat{K}_A) = C \underline{E}_{Tff} \cdot \hat{n}_b \quad (2)$$

where C is a complex constant and  $\hat{n}_b$  is a generally complex vector which describes the orientation and polarization of an infinitesimal current element located in the direction (with respect to the antenna) given by  $\hat{K}_A$ . Equation (2) provides the connection between the receiving and transmitting formulations and is the third facet of a basic theory of radome analysis.

### Application

A computationally fast method of radome analysis based on a receiving formulation results when the surface  $S$  in Equation (1) is chosen to coincide with the planar aperture of the antenna whose radiating characteristics are represented using the plane wave spectrum formulation. The receiving pattern (difference channel) in the azimuth plane for a vertically polarized antenna with square aperture (corners removed) of dimensions  $4.3\lambda \times 4.3\lambda$  is shown in Figure 2 for the case of a Pyroceram radome of wall thickness  $d = .22\lambda$ . The tangent ogive radome with fineness ratio  $L/D = 2.25$  is gimballed so that its tip is positioned at  $+12^\circ$  in the azimuth plane of the antenna. Execution time to generate this pattern and three others like it was 104 seconds (CDC Cyber 70).

For comparison, the pattern obtained for the same values of radome and antenna parameters when a transmitting formulation is used is shown in Figure 3. In this method, a PWS representation is used to describe the antenna, and rays representing each plane wave are used to construct an equivalent aperture which includes the effects of the radome on each plane wave in the spectrum. The execution time to generate this pattern and three others was 60 seconds on the same computing system.

Other methods of analysis which utilize integration on the surface of the radome for both receiving and transmitting formulations are currently being implemented. Computed results obtained using these methods will be presented at the symposium. The experimental procedures being used will also be described.

### Acknowledgement

This research is sponsored by the Air Force Office of Scientific Research, Air Force Systems Command, USAF, under Grant No. AFOSR-77-3469. The United States Government is authorized to reproduce and distribute reprints for governmental purposes notwithstanding any copyright notation hereon.

### References

1. R. E. Collin and F. J. Zucker, "Antenna Theory, Part 1," Section 4.2, McGraw-Hill, New York, 1969.
2. Ibid., Section 3.3.
3. S. Silver, ed., "Microwave Antenna Theory and Design," Section 3-8, McGraw-Hill, New York, 1949.
4. Collin and Zucker, op. cit., Section 4.5.

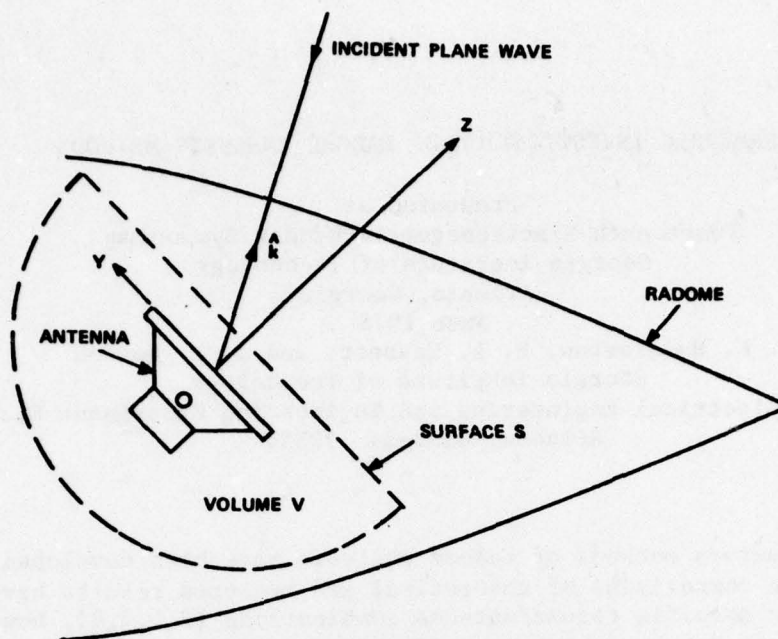


FIGURE 1. ANTENNA/RADOME GEOMETRY FOR ANALYSIS.

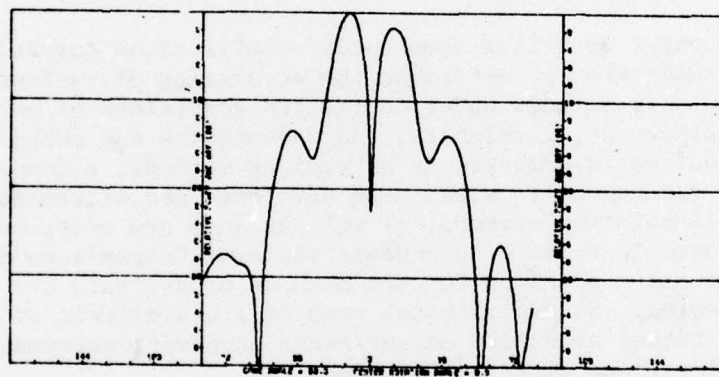


FIGURE 2. AZIMUTH PATTERN FOR RECEIVING FORMULATION.

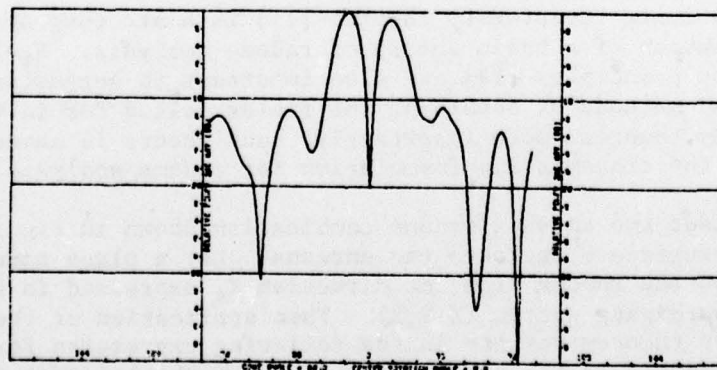


FIGURE 3. AZIMUTH PATTERN FOR TRANSMITTING FORMULATION.

## PARAMETRIC INVESTIGATION OF RADOME ANALYSIS METHODS

Presented at  
Fourteenth Electromagnetic Window Symposium  
Georgia Institute of Technology  
Atlanta, Georgia  
June 1978

G. K. Huddleston, H. L. Bassett, and J. M. Newton  
Georgia Institute of Technology  
School of Electrical Engineering and Engineering Experiment Station  
Atlanta, Georgia 30332

Numerous methods of radome analysis have been developed [1-9], and some comparisons of theoretical and measured results have been made for specific radome/antenna combinations [2,5,7,8]; however, no attempt has been made to define the ranges of antenna and radome parameters over which any given method of analysis yields acceptably accurate results.

This paper describes some early results of an investigation recently undertaken to determine the accuracies of various radome analysis methods under controlled conditions of antenna size and placement, wavelength, and radome size and shape. To carry out valid comparisons of various methods, a fundamental theory of radome analysis has been developed and is presented below. All existing methods, as well as some new ones, can be formulated in terms of the basic theory. Comparisons of computed results obtained for two methods of analysis are also presented. No experimental results are available at this time, but rather extensive measurements involving antennas and radomes of various sizes are planned.

### Theory

The Lorentz reciprocity theorem [11] is a starting point for the formulation of a basic theory of radome analysis. Field equivalence principles [12] are also important in suggesting approximate methods of obtaining the fields called for in the reciprocity theorem; more importantly, such theory is needed to obtain the transmitting formulation for radome analysis.

Consider the antenna/radome combination shown in Figure 1 where the surface  $S$  encloses the antenna. Let a plane wave be incident on the radome from the direction  $K_A$  expressed in the antenna coordinate system  $(X,Y,Z)$ . Then application of the reciprocity theorem results in the following expression for the voltage produced at the antenna terminals by the incident field:

$$V_R (\hat{K}_A) = C \int \int_S (\underline{E}_T \times \underline{H}_R - \underline{E}_R \times \underline{H}_T) \cdot \hat{n} da \quad (1)$$

where C is a complex constant and where

$\underline{E}_T, \underline{H}_T$  = the electric and magnetic fields produced on S when the antenna is transmitting (and no fields are incident on the radome from the outside)

$\underline{E}_R, \underline{H}_R$  = the electric and magnetic fields produced on S when the plane wave is incident (and the antenna is passive or in the receive mode)

$\hat{n}$  = unit vector pointing out of the volume V enclosed by S

da = element of area on the surface S

The fields  $(\underline{E}_R, \underline{H}_R)$  and  $(\underline{E}_T, \underline{H}_T)$  are the total fields produced in each case and would correctly include incident and all scattered components. The voltage given by Equation (1) is exact and serves as a basic tenet of radome analysis theory. The surface S may be any conveniently chosen closed surface. Linear, homogenous, isotropic media are assumed. Time variations of the form  $e^{j\omega t}$  are understood and suppressed.

The selection of the surface S and the approximations used to determine the fields  $(\underline{E}_T, \underline{H}_T)$  and  $(\underline{E}_R, \underline{H}_R)$  on this surface are the parameters which differentiate the various methods of radome analysis which are based on a receiving formulation. For example, Tricoles [5] and Huddleston and Joy [10] chose a planar surface coinciding with the antenna aperture for the surface S, ignoring the contribution of that portion of the surface needed to completely enclose the antenna. Huddleston and Joy used ray tracing to approximate the fields  $(\underline{E}_R, \underline{H}_R)$  on S. Tricoles used field equivalence and induction theorems to determine these fields on S. Huddleston and Joy used the primary transmitting fields of the antenna to approximate  $(\underline{E}_T, \underline{H}_T)$ . Tricoles used measured values of antenna response.

Other approximate methods based on the receiving formulation in Equation (1) are obvious. Consider the surface S which coincides with the inner surface of the radome. The fields  $(\underline{E}_T, \underline{H}_T)$  on S may be approximated using modal expansions such as the PWS [8], a spherical wave expansion [13], or from theoretical analysis [14]. These fields should correctly contain reflected components which may be approximated using plane sheet transmission coefficients and Poynting's vector. The fields  $(\underline{E}_R, \underline{H}_R)$  on S may be approximated using plane sheet transmission coefficients and ray tracing. The voltage received could then be obtained by performing the surface integration over the inside surface of the radome indicated by Equation (1).

The effects of reflections may also be included in the analysis. Let  $(\underline{E}_T', \underline{H}_T')$  represent the transmitting fields on the surface S which coincides with the inner radome surface. Then at a point P on the inner surface, the fields at all other points contribute components due to reflections given by [15]

$$\underline{E}_P = \frac{1}{4\pi} \iint_S [-j\omega\mu \psi (\hat{n} \times \underline{H}_T') + (\hat{n} \times \underline{E}_T') \times \nabla\psi + (\hat{n} \cdot \underline{E}_T') \nabla\psi] dS \quad (2)$$

$$\underline{H}_P = \frac{1}{4\pi} \iint_S [j\omega\epsilon (\hat{n} \times \underline{E}_T') \psi + (\hat{n} \times \underline{H}_T') \times \nabla\psi + (\hat{n} \cdot \underline{H}_T') \nabla\psi] dS \quad (3)$$

where

$$\psi = \frac{e^{-jkr}}{r} \quad (4)$$

and where r is the distance from P to any other point on S. The importance of the contributions of first and higher order reflections has not been established.

A second generalized approach to radome analysis uses a transmitting formulation which does not consider explicitly the fields produced by an incident plane wave. Instead, the tangential fields produced by the antenna on a closed surface outside the radome are used to determine the fields anywhere in the unbounded, homogenous medium outside this surface. Equations (2) and (3) are the basic equations which apply, where the point P is at a great distance from S so that  $\underline{E}_P, \underline{H}_P$  become the far zone fields  $\underline{E}_{Tff}, \underline{H}_{Tff}$  radiated by the antenna in the presence of the radome. Selection of the surface S and the approximations used to find the fields  $(\underline{E}_T, \underline{H}_T)$  on S are the parameters which, again, differentiate the various methods of radome analysis based on a transmitting formulation.

The voltage that would be received by the antenna which produces far zone fields  $\underline{E}_{Tff}, \underline{H}_{Tff}$  is given by [23]

$$V_R(\hat{K}_A) = C \underline{E}_{Tff} \cdot \hat{n}_b \quad (5)$$

where C is a complex constant and  $\hat{n}_b$  is a generally complex vector which describes the orientation and polarization of an infinitesimal current element located in the direction given by  $\hat{K}_A$ . Note that the current element would produce an

incident plane wave on the radome having the same polarization as that indicated by  $\hat{n}_b$ ; hence, Equation (5) provides the connection between the receiving and transmitting formulations and is a third facet of a basic theory of radome analysis.

The above equations combine to form a fundamental theory of radome analysis. All existing analysis methods, as well as some new ones, can be cast in terms of this theory. The theory provides a rigorous framework in which the approximations which may be used in any analysis method can be clearly seen and their effects on predicted results assessed. Comparisons of the various methods in terms of speed of computations and accuracy can also be made.

All radome analysis methods of practical interest entail approximations of one form or another. Consequently, the only satisfactory way to determine the accuracy of any method is by comparison with experimental data. To cover the broad range of parameters that may be encountered in practice, combinations of radomes and antennas of various sizes should be carefully selected for measurement to yield the most useful true data for assessing the accuracies of different methods of analysis.

#### Application

A computationally fast method of radome analysis based on a receiving formulation [10] results when the surface  $S$  in Equation (1) is chosen to coincide with the planar aperture of the antenna whose radiating characteristics are represented using the plane wave spectrum formulation [17]. The difference receiving pattern in the azimuth plane for a vertically polarized monopulse antenna with square aperture (corners removed) of dimensions  $4.3\lambda \times 4.3\lambda$  is shown in Figure 2 for the case of a Pyroceram radome of wall thickness  $d = .22\lambda$ . The tangent ogive radome with fineness ratio  $L/D = 2.25$  gimbaled so that its tip is positioned at  $+12^\circ$  in the azimuth plane of the antenna. Execution time to generate this pattern and three others like it was 104 seconds (CDC Cyber 70).

For comparison, the pattern obtained for the same values of radome and antenna parameters when a transmitting formulation [9] is used is shown in Figure 3. In this method, a PWS representation is used to describe the antenna, and rays representing each plane wave are used to construct an equivalent aperture which includes the effects of the radome on each plane wave in the spectrum. The execution time to generate this pattern and three others was 60 seconds on the same computing system.

Other methods of analysis which utilize integration on the surface of the radome for both receiving and transmitting formulations are currently being implemented. Computed results obtained using these methods will be presented at the symposium. The

experimental procedures being used will also be described.

#### Summary

A fundamental theory of radome analysis, which embodies all existing methods as well as some new ones, is presented. Computed results using two different methods of analysis have been obtained as preliminary data. Computed results obtained using additional methods of analysis will be presented at the symposium.

#### Acknowledgement

This research is sponsored by the Air Force Office of Scientific Research, Air Force Systems Command, USAF, under Grant No. AFOSR-77-3469. The United States Government is authorized to reproduce and distribute reprints for governmental purposes notwithstanding any copyright notation hereon.

#### References

1. "Microwave Antenna Theory and Design," edited by Samuel Silver, McGraw-Hill Book Company, Chapter 14, 1949.
2. N. R. Kilcoyne, "An Approximate Calculation of Radome Boresight Error," Proceedings of the USAF/Georgia Institute of Technology Symposium on Electromagnetic Windows, pp. 91-111, June 1968.
3. O. Snow, "Discussion of Ellipticity Produced by Radomes and Its Effects on Crossover Point Position for Conically Scanning Antennas," U. S. Naval Air Development Center, Report E15108, 1951.
4. P. I. Pressel, "Boresight Prediction Technique," Proceedings OSU-WADC Radome Symposium, 1956.
5. G. Tricoles, "Radiation Patterns and Boresight Error of a Microwave Antenna Enclosed in an Axially Symmetric Dielectric Shell," J. Optical Soc. of America, 54, No. 9, pp. 1094-1101, September 1964.
6. M. Tavis, "A Three-Dimensional Ray Tracing Method for the Calculation of Radome Boresight Error and Antenna Pattern Distortion," Report No. TOR-0059(56860)-2, Air Force Systems Command, May 1971.
7. D. T. Paris, "Computer-Aided Radome Analysis," IEEE Transactions, AP-18, No. 1, pp. 7-15, January 1970.

8. D. C. F. Wu and R. C. Rudduck, "Application of Plane Wave Spectrum Representation to Radome Analysis," Proceedings of the Tenth Symposium on Electromagnetic Windows, pp. 46-49, July 1970; also Final Technical Report 2969-4 (AD 722 634), March 1971.
9. E. B. Joy and G. K. Huddleston, "Radome Effects on Ground Mapping Radar," Contract DAAH01-72-C-0598, U. S. Army Missile Command, March 1973.
10. G. K. Huddleston and E. B. Joy, "Development of Fabrication and Processing Techniques for Laser Hardened Missile Radomes: Radome Electrical Design Analysis," MMC Purchase Agreement No. 573712, Martin Marietta Aerospace, March 1977.
11. R. E. Collin and F. J. Zucker, "Antenna Theory, Part 1," Section 4.2, McGraw-Hill Book Company, New York, 1969.
12. Ibid., Section 3-3.
13. A. C. Ludwig, "Near-Field Far-Field Transformations Using Spherical Wave Expansions," IEEE Transactions, AP-19, No. 2, pp. 214-220, March 1971.
14. D. T. Paris, "Digital Computer Analysis of Aperture Antennas," IEEE Transactions, AP-16, pp. 262-264, March 1968.
15. Silver, op. cit., Section 3-8, Equations (108)-(109).
16. Collin and Zucker, op.cit., Section 4.5.
17. H. G. Booker and P. C. Clemmow, "The Concept of an Angular Spectrum of Plane Waves, etc.," Proceedings IEE, 97, Part III, p. 11-17, 1950.

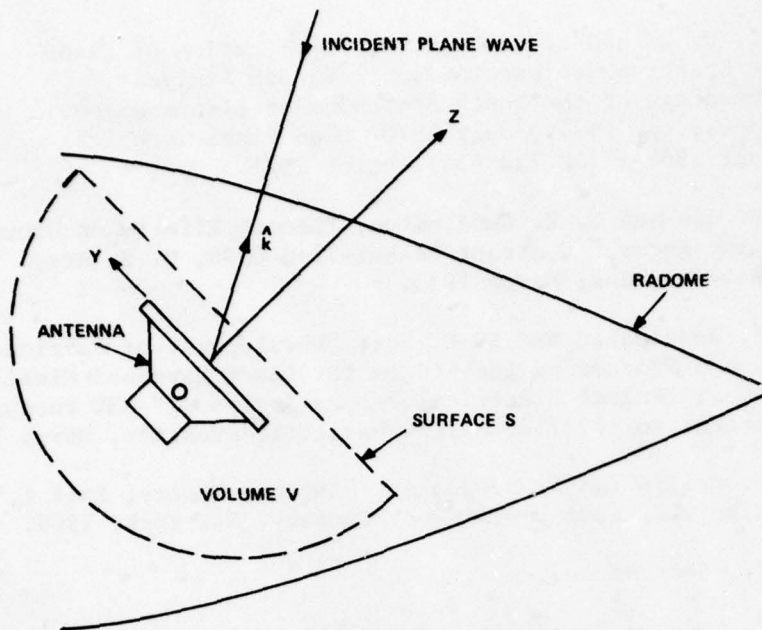


FIGURE 1. ANTENNA/RADOME GEOMETRY FOR ANALYSIS.

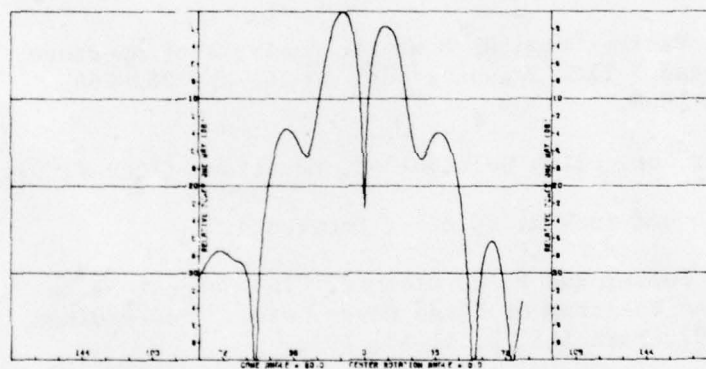


FIGURE 2. AZIMUTH PATTERN FOR RECEIVING FORMULATION.

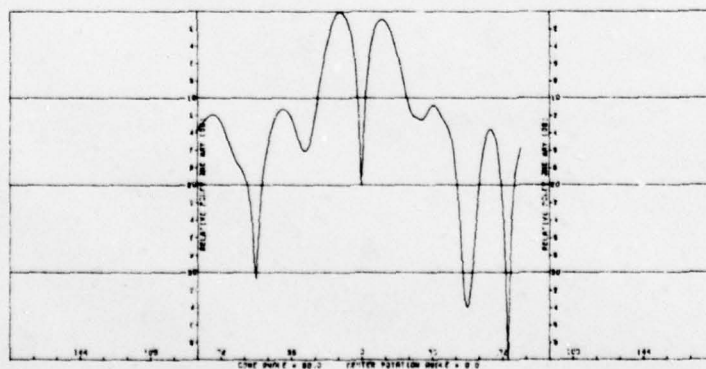


FIGURE 3. AZIMUTH PATTERN FOR TRANSMITTING FORMULATION.

UNCLASSIFI.

SECURITY CLASSIFICATION OF THIS (When Data Entered)

19 REPORT DOCUMENTATION PAGE		READ INSTRUCTIONS BEFORE COMPLETING FORM
1. REPORT NUMBER <b>AFOSR/TR-79-0068</b>	2. GOVT ACCESSION NO.	3. RECIPIENT'S CATALOG NUMBER
4. TITLE (and Subtitle) Parametric Investigation of Radome Analysis Methods	5. TYPE OF REPORT & PERIOD COVERED Interim October 1, 1977 to Sept. 30, 1978	
6. AUTHOR(s) G. K. Huddleston, H. L. Bassett, and J. N. Newton	6. PERFORMING ORG. REPORT NUMBER	
7. PERFORMING ORGANIZATION NAME AND ADDRESS Georgia Institute of Technology School of Electrical Engineering Atlanta, Georgia 30332	8. CONTRACT OR GRANT NUMBER(s) AFOSR-77-3469	
9. CONTROLLING OFFICE NAME AND ADDRESS Air Force Office of Scientific Research Directorate of Physics/NP Bolling Air Force Base, D.C. 20332	10. PROGRAM ELEMENT, PROJECT, TASK AREA & WORK UNIT NUMBERS 61102F 16 2301/A6 17 A6	
11. MONITORING AGENCY NAME & ADDRESS (if different from Controlling Office) Annual technical rept. 1 Oct 77 - 30 Sep 78	12. REPORT DATE November 30, 1978	
	13. NUMBER OF PAGES 40	
	14. SECURITY CLASS. (of this report) Unclassified 12 42p.	
15. DECLASSIFICATION/DOWNGRADING SCHEDULE		
15. DISTRIBUTION STATEMENT (of this Report)  Approved for public release; distribution unlimited.		
17. DISTRIBUTION STATEMENT (of the abstract entered in Block 20, if different from Report)		
18. SUPPLEMENTARY NOTES		
19. KEY WORDS (Continue on reverse side if necessary and identify by block number)  Radome Analysis Millimeter Wave Radomes		
20. ABSTRACT (Continue on reverse side if necessary and identify by block number)  The status is described of a research program whose objective is to determine the accuracies of various methods of radome analysis as functions of antenna size and placement, radome size and shape, and wavelength. The analytical methods used and the experimental program to establish true data are described concisely.		

408 631

JOB